

## Entanglement dynamics for a conditionally kicked harmonic oscillator

This content has been downloaded from IOPscience. Please scroll down to see the full text.

2016 J. Phys. B: At. Mol. Opt. Phys. 49 165501

(<http://iopscience.iop.org/0953-4075/49/16/165501>)

View [the table of contents for this issue](#), or go to the [journal homepage](#) for more

### Download details:

IP Address: 178.250.250.21

This content was downloaded on 29/09/2016 at 05:23

Please note that [terms and conditions apply](#).

You may also be interested in:

[An Introduction to the Formalism of Quantum Information with Continuous Variables: Quantum information with continuous variables](#)

C Navarrete-Benlloch

[Quantum and classical control of single photon states via a mechanical resonator](#)

Sahar Basiri-Esfahani, Casey R Myers, Joshua Combes et al.

[Entanglement dynamics in a two-mode nonlinear bosonic Hamiltonian](#)

L Sanz, R M Angelo and K Furuya

[Efficient and exact numerical approach for many multi-level systems in open system CQED](#)

Michael Gegg and Marten Richter

[From quantum to classical: Schrödinger cats, entanglement, and decoherence](#)

L Davidovich

[Universal quantum computation in waveguide QED using decoherence free subspaces](#)

V Paulisch, H J Kimble and A González-Tudela

[Decoy-state quantum key distribution with a leaky source](#)

Kiyoshi Tamaki, Marcos Curty and Marco Lucamarini

# Entanglement dynamics for a conditionally kicked harmonic oscillator

Eric G Arrais<sup>1</sup>, J S Sales<sup>2</sup> and N G de Almeida<sup>1,3</sup>

<sup>1</sup>Instituto de Física, Universidade Federal de Goiás, 74.001-970, Goiânia (GO), Brazil

<sup>2</sup>Unucet, Universidade Estadual de Goiás, 75132-903, Anápolis (GO), Brazil

E-mail: [norton@ufg.br](mailto:norton@ufg.br)

Received 19 January 2016, revised 25 May 2016

Accepted for publication 24 June 2016

Published 29 July 2016



## Abstract

The time evolution of the quantum kicked harmonic oscillator (KHO) is described by the Floquet operator which maps the state of the system immediately before one kick onto the state at a time immediately after the next. Quantum KHO is characterized by three parameters: the coupling strength  $V_0$ , the so-called Lamb–Dicke parameter  $\eta$  whose square is proportional to the effective Planck constant  $\hbar_{\text{eff}}$ , and the ratio  $T$  of the natural frequency of the oscillator and the kick frequency. To a given coupling strength and depending on  $T$  being a natural or irrational number, the phase space of the classical kicked oscillator can display different behaviors, as for example, stochastic webs or quasicrystal structures, thus showing a chaotic or localized behavior that is mirrored in the quantum phase space. On the other hand, the classical limit is studied letting  $\hbar_{\text{eff}}$  become negligible. In this paper we investigate how the ratio  $T$ , considered as integer, rational or irrational, influences the entanglement dynamics of the quantum KHO and study how the entanglement dynamics behaves when varying either  $V_0$  or  $\hbar_{\text{eff}}$  parameters.

**Keywords:** entanglement dynamics, entanglement in kicked systems, conditional kicked harmonic oscillator

(Some figures may appear in colour only in the online journal)

## 1. Introduction

Quantum kicked oscillators have attracted a lot of attention, mainly because kicked Hamiltonian systems are well-suited models for studying quantum chaos [1–4, 20, 21]. The quantum kicked *harmonic* oscillator (KHO) model, in turn, has been studied in several contexts, for example for electronic transport in semiconductor superlattices [6], atom optic modeling using ion traps [7, 18], and Bose–Einstein condensate in a harmonic confinement [5, 11]. Recently, several theoretical works considering KHO have appeared. Particularly, in [10], the authors study the role of both the macroscopic limit and the different system–environment interactions in the quantum to classical transition of a chaotic system. In [18] the authors showed that the atom-optical KHO displays quantum resonances dependent on the value of the squared Lamb–Dicke parameter. In [5] the authors presented

a treatment of a Bose condensate driven by an external temporally periodic force, controlling the dynamics of the system. In [17] the authors showed that the heating of harmonically trapped ions by periodic delta kicks can be enhanced for some values of the Lamb–Dicke parameter. Also, some experimental work on quantum kicked oscillators was carried out in the context of atoms [3, 19, 20], Bose–Einstein condensates [22], and photonics lattices [23]. Particularly, in [7], the authors introduced a conditional quantum KHO, in the context of trapped ions, and showed how to directly measure the sensitivity of the ion motion to small variations of external parameters. Experimental realizations of quantum KHO, on the other hand, are rather scarce, and recently it was implemented in the spatial degrees of freedom of the photons of a monochromatic paraxial light [24], and even for a few number of kicks.

The main parameters dictating the dynamics of the quantum KHO, given by the Floquet operator, is the coupling strength  $V_0$ , the effective Planck constant,  $\hbar_{\text{eff}}$ , which is

<sup>3</sup> Author to whom any correspondence should be addressed.

related to the Lamb–Dicke parameter  $\eta$  as  $\hbar_{\text{eff}} \propto \eta^2$ , and the ratio  $T$  between the natural frequency  $\omega$  of the system and the kicking frequency  $\omega_k$ . It is well known that depending on this ratio  $T$  being integer, rational or irrational, the quantum KHO phase space (Husimi or Wigner functions) can display very different behaviors, such as stochastic web with crystal or quasi-crystal symmetry [7, 8, 17, 18]. Also, transition from quantum to classical chaos can be studied by progressively reducing  $\hbar_{\text{eff}}$  [7]. In this paper we take advantage of the conditional quantum KHO, as introduced in [7], to study the dynamics of entanglement being created when the conditional kicked is applied to initial product states for different ratios  $T$ , strengths  $V_0$  and effective Planck constants  $\hbar_{\text{eff}}$ . As we shall see, there are distinct behaviors to the entanglement, depending on the values of  $T$ ,  $V_0$ , and  $\hbar_{\text{eff}}$ .

## 2. The model

Similarly to [7], we will follow the dynamics of our system given by the KHO using as ancilla (B) a two-level system, and write explicitly the effective Hamiltonian  $H = H_0 + V$ , with

$$H_0 = \hbar\omega \left( a^\dagger a + \frac{1}{2} \right) \quad (1)$$

$$V = V_0 \cos[\eta(a + a^\dagger)] |0\rangle_B \langle 0| \sum_{n=-\infty}^{\infty} \delta(t - n\tau), \quad (2)$$

where  $\omega$  is the (unkicked) oscillator frequency,  $\tau$  is the interval between two consecutive kicks,  $V_0$  is the coupling strength,  $a^\dagger$  and  $a$  are respectively the creation and annihilation bosonic operators,  $|0\rangle \langle 0|$  is one of two two-states of a qubit lying in the Hilbert space  $\{|0\rangle_B, |1\rangle_B\}$ , and  $\eta = k\sqrt{\hbar/2m\omega}$  is the Lamb–Dicke parameter, with  $m$  being the mass of the oscillator. Note, by the very definition of the Lamb–Dicke parameter, that  $\eta^2 \propto \hbar_{\text{eff}}$ . This model can be accomplished within an ion trap subjected to a sequence of standing-wave laser pulses, where  $|0\rangle \langle 0|$  is one of two electronic states of a two-level trapped ion [7]. As the standing wave has the shape  $\mathbf{E} \cos(\mathbf{k} \cdot \mathbf{r} + \phi)$ , where  $\mathbf{k}$  is the wave vector and  $\phi$  is a phase indicating the position of the ion in the standing wave, this model can be accomplished placing the ion on the standing-wave antinode ( $\phi = 0$ ). Note therefore that  $\cos[\eta(a + a^\dagger)]$  comes from  $\mathbf{k} \cdot \mathbf{x}$ , meaning that the interaction Hamiltonian has a nonlinear dependence on the position of the harmonic oscillator. Also, it is worthwhile mentioning that recent achievements in the growing field of optomechanics, including hybrid optomechanical oscillators with embedded quantum two-level systems [12–15], which could be used as the ancilla, would enable the realization of this model in that context as well.

The time evolution to this conditional KHO is given by the conditional-Floquet operator, which, for computational

convenience, we write as

$$\mathcal{F} = \exp \left[ -iT \left( a^\dagger a + \frac{1}{2} \right) \right] \times \exp \left\{ -i \frac{V_0}{\hbar} \cos[\eta(a + a^\dagger)] |0\rangle_B \langle 0| \right\} \equiv U_0 U_k \quad (3)$$

where  $T = 2\pi\omega/\omega_k$  is the ratio between the natural frequency of the system  $\omega$  and the kicking frequency  $\omega_k$ . This ratio, as well as the strength of the kicking potential, determines the global dynamics of the quantum OHK [8]. Note that  $T = N\pi$ ,  $N = 2, 4, 6, \dots$  corresponds to cases where the frequency of the harmonic oscillator is an integer multiple of the kick frequencies. In particular,  $T = \pi$  corresponds to a frequency of kicks that is twice that of the oscillator.

*Quantum correlations:* to investigate entanglement dynamics to the conditioned delta-kicked harmonic oscillator (KHO), we will use local quantum uncertainty (LQU) [25]. LQU was recently proposed as a measure of quantum correlations for bipartite quantum systems ( $A$  and  $B$ ) and is defined as

$$LQU(\rho) = \min_{K_A} I(\rho, K_A), \quad (4)$$

where the minimization runs over all the non-degenerate observables  $K_A = K_A \otimes \mathbf{I}_B$  on system  $A$  and  $I(\rho, K) = -\frac{1}{2} \text{tr}[\rho^{1/2}, K]^2$  is the skew information [16]. It can be shown that LQU, as defined above, satisfies all the physical requirements of a measure of quantum correlations, thus being entanglement monotonic for pure states, invariant under local unitary operations, non increasing under local operations, and vanishing if and only if the quantum state is of zero discord under measurements on  $A$ .

For a two-level system, LQU of system  $A$  is calculated by solving  $U_A(\rho_{AB}) = 1 - \lambda_{\max}\{W_{AB}\}$ , where  $\lambda_{\max}\{W_{AB}\}$  denotes the maximum eigenvalue of the matrix  $W_{AB}$  whose elements are  $(i, j = x, y, z)$ :

$$(W_{AB})_{ij} = \text{tr} \left\{ (\rho_{AB})^{\frac{1}{2}} (\sigma_{iA} \otimes I_B) (\rho_{AB})^{\frac{1}{2}} (\sigma_{jA} \otimes I_B) \right\}. \quad (5)$$

LQU main advantages, compared to other measures of quantum correlations, is that it does not require optimization procedures and recover linear entropy for pure states [25].

We assume as initial condition the state

$$|\Psi(0)\rangle_{AB} = \frac{(|\phi\rangle_A |0\rangle_B + |\gamma\rangle_A |1\rangle_B)}{\sqrt{2}}, \quad (6)$$

where  $|\phi\rangle_A$  and  $|\gamma\rangle_A$  are the states of the KHO and  $|0\rangle_B$  ( $|1\rangle_B$ ) is de ground (excited) state of a single trapped ion. After  $n$  kicks the result will be the entangled state

$$|\Psi(n\tau)\rangle = \frac{(F^n |\phi\rangle_A |0\rangle_B + U_0^n |\gamma\rangle_A |1\rangle_B)}{\sqrt{2}}, \quad (7)$$

where  $F^n = \left[ \exp \left[ -iT \left( a^\dagger a + \frac{1}{2} \right) \right] \exp \left[ -i \frac{V_0}{\hbar} \cos [\eta (a + a^\dagger)] \right] \right]^n$ , with the corresponding density operator

$$\begin{aligned} \rho_{AB}(t) = & \frac{1}{2} [ |1\rangle_B \langle 1| U_0^n |\gamma\rangle_A \\ & \times \langle \gamma| U_0^{\dagger n} + |0\rangle_B \langle 0| F_n |\phi\rangle_A \langle \phi| F_n^\dagger \\ & + |0\rangle_B \langle 1| F_n |\phi\rangle_A \langle \gamma| U_0^{\dagger n} \\ & + |1\rangle_B \langle 0| U_0^n |\gamma\rangle_A \langle \phi| F_n^\dagger ]. \end{aligned} \quad (8)$$

We can now trace out the KHO system (A) to obtain the reduced operator for the ancilla

$$\begin{aligned} \rho_B(t) = & \frac{1}{2} [ \mathbf{1}_B + {}_A \langle \gamma| U_0^{\dagger n} F^n |\phi\rangle_A |0\rangle_B \langle 1| \\ & + {}_A \langle \phi| F^{n\dagger} U_0^n |\gamma\rangle_A |1\rangle_B \langle 0| ]. \end{aligned} \quad (9)$$

and also

$$\text{tr} \rho_B^2(t) = \frac{1}{2} + \frac{1}{2} |{}_A \langle \phi| F^{n\dagger} U_0^n |\gamma\rangle_A|^2, \quad (10)$$

Entanglement can now be easily computed. Since we are dealing with pure states, the LQU is calculated through the linear entropy [25]

$$LQU(|\Psi(n\tau)\rangle_{AB} \langle \Psi(n\tau)|) = 2[1 - \text{tr}(\rho_A)^2] \quad (11)$$

$$LQU(|\Psi(n\tau)\rangle_{AB} \langle \Psi(n\tau)|) = [1 - |{}_A \langle \phi| F^{n\dagger} U_0^n |\gamma\rangle_A|^2]. \quad (12)$$

We do not attempt to solve this problem analytically. While some progress have been made for the Floquet operator acting on the coherent state [18], even for few kicks these generally involve a formidable task, needing to deal with infinite summations of Bessel functions, which leads to excessive complications turning virtually impossible to extract useful information on the dynamics of the quantum KHO [8]. Instead, we investigate numerically the behavior of LQU considering, as said previously, different ratios  $T$ , parameters  $\hbar_{\text{eff}}$ , and strengths  $V_0$ . As for example, resonance conditions occur for  $T_{\text{RES}} = 2\pi/q$ , with  $q \in \mathbb{N}$ . Periodic webs, which are characterized by both rotational and translational symmetries, is expected to occur for  $q = 1, 2, 3, 4, 6$ . On the other hand, the nonresonant kicked harmonic oscillator can exhibit Anderson localization, depending on the match of some parameters of the model [9], and the crystalline structure disappears in the classical phase plane when  $T$  is irrational [8]. Also, we study how entanglement evolves when the parameter  $V_0$  is either increased or decreased. Finally, as entanglement is a purely quantum phenomenon, it is interesting to verify what happens in the limit  $\hbar_{\text{eff}} \rightarrow 0$ .

### 3. Numerical results

Let us first consider as the initial state of the KHO a coherent state, such that  $|\gamma\rangle_A = |\phi\rangle_A = |\alpha\rangle_A$ , thus meaning that the initial entanglement is null. We start by investigating the conditional Floquet operator's ability to create entanglement when different ratios  $T$  are taken into account. For this, in

figures 1 to 4 we keep fixed  $\eta = 1/\sqrt{2}$ ,  $V_0 = 0.25$ ,  $\alpha = \beta = 5$ . We start plotting LQU versus number of kicks, figure 1, varying  $T = \pi, 4, 5, 6$ . Note that while entanglement is enhanced for  $T = \pi$ , becoming near unity for few kicks, it increases near linearly for the integers  $T = 4, 5, 6$ . This could suggest that entanglement grows faster for irrational ratios, but, interestingly, this is not always true: there are some irrationals for which entanglement increases as slowly as those integers, as can be seen in figure 2, where we plot entanglement versus number of kicks for irrational rates  $T = \sqrt{2}, (\sqrt{5} + 1)/2, e$ . For comparison, we also show entanglement for  $T = \pi$ , as before. Figures 1 and 2 look very similar, and it is easy to see that the ratio  $T = \pi$  stands out from the other irrational ratios. This ability to rapidly create entanglement when  $T = p\pi$ ,  $p = 1, 2, 3, \dots$ , as compared to other values of  $T$ , is manifested for other initial states, as for example for the product of the ancilla and Fock state, such that  $|\gamma\rangle_A = |\phi\rangle_A = |n\rangle_A$ , where  $|n\rangle_A$  is the Fock state. To see this, in figure 3 we consider the Fock state  $|10\rangle_A$ , when plotting LQU versus number of kicks, to the same parameter as before. Note how the rate  $T = \pi$  stands out from the others ratios, no matter if integer, rational or irrational. Also interesting is the fact that there exist some multiple of  $\pi$ , in fact,  $T = p\pi$ , that enhances entanglement after few kicks. Also, note that when the kick frequency becomes too high as compared to the natural frequency,  $T = 2\pi\omega/\omega_k \rightarrow 0$ , entanglement is generated and affected only by the kick term of equation (3). According to our numerical simulations (not shown), when fixing the other parameters, all the curves overlap for  $T = p\pi$ ,  $p = 1, 2, 3, \dots$ . On the other hand, as shown in figure 4, where we show entanglement versus number of kicks for the same parameters used in figure 3, while integer multiples of  $\pi$  always enhance entanglement, rational multiples stop to enhance entanglement for  $p < 1/3$ , (see legend in figure 4). Although this behavior changes quantitatively depending on the initial states as well as the set of parameters, according to our numerical simulations with Fock and coherent states, if the parameters  $V_0$  and  $\hbar_{\text{eff}}$  are kept unchanged, qualitatively this behavior remains the same.

Clearly, from figure 4, we see that when  $T = \pi/3$  (green) there are a steady increasing of entanglement: for  $p < 1/3$  entanglement increases slowly, while for  $p > 1/3$  entanglement increases rapidly as compared to the other ratios  $T$ . Also, note that for  $T = \pi/2$  (red) entanglement falls appreciably for  $N > 30$  kicks. We could ask if it will start to increase again, or rather will keep falling. Numerical simulations with  $N = 200$  indicate an oscillatory behavior where LQU attains a minimum (approximately 0.4) returning to high values (approximately 0.9).

Now we investigate how entanglement evolves when the coupling strength  $V_0$  is either increased or decreased. To this, we keep the Lamb-Dicke parameter fixed at  $\eta = 1/\sqrt{2}$  and the rate  $T = \pi$ , which, as we have shown, optimizes the entanglement, considering initially a product of the ancilla and coherent state  $|\gamma\rangle_A = |\phi\rangle_A = |\alpha\rangle_A$ . As our numerical simulations show, the amplitude of the coherent state being real or complex has little influence on the LQU behavior, so we choose  $\alpha = 2$ . As can be seen in figure 5, entanglement

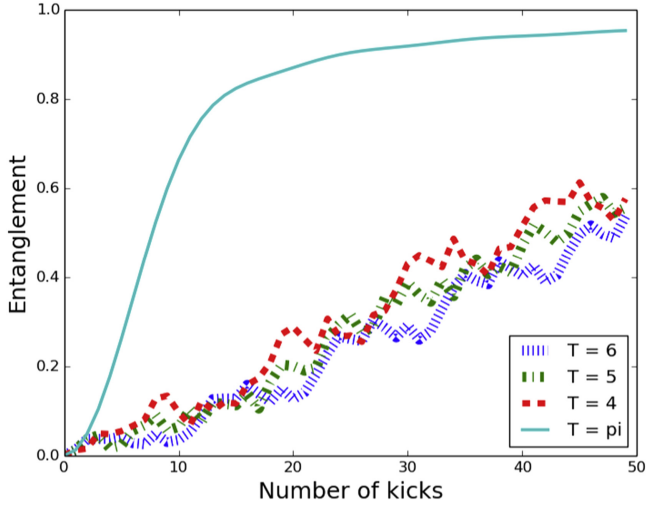


**Figure 1.** Entanglement versus number of kicks for  $\eta = 1/\sqrt{2}$ ,  $V_0 = 0.25$ ,  $T = \pi$  (cyan),  $T = 4$  (blue),  $T = 5$  (green), and  $T = 6$  (red). The initial state was taken as a product of the ancilla and coherent state with  $\alpha = 5$ .

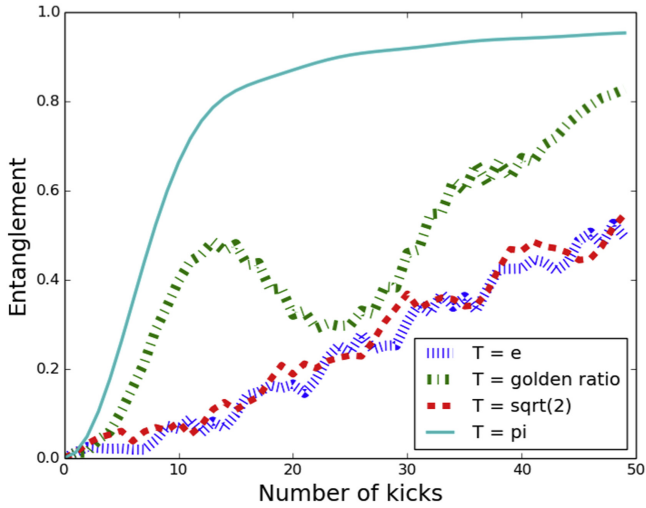


**Figure 2.** Entanglement versus number of kicks for  $\eta = 1/\sqrt{2}$ ,  $V_0 = 0.25$ ,  $T = \pi$  (cyan),  $T = \sqrt{2}$  (blue),  $T = (\sqrt{5} + 1)/2$  (green), and  $T = \exp(1)$  (red). The initial state was taken as a product of the ancilla and coherent state with  $\alpha = 5$ .

increases and starts to oscillate faster for increasing values of  $V_0$ . It is to be noted, however, that in our numerical simulations (not shown) we found that, for this initial coherent state, if  $V_0 \gtrsim 10$ , the maximum entanglement is attained for few kicks regardless of the rate  $T$ .

Finally, we investigate how entanglement behaves with  $\hbar_{\text{eff}}$ . To do this, following [7, 24] we rewrite the conditional Floquet operator, equation (4), as

$$\mathcal{F} = \exp\left[-iT\left(a^\dagger a + \frac{1}{2}\right)\right] \times \exp\left\{-i\frac{V_0}{\hbar_{\text{eff}}} \cos\left[\sqrt{\frac{\hbar_{\text{eff}}}{2}}(a + a^\dagger)\right] |0\rangle_B \langle 0|\right\}. \quad (13)$$

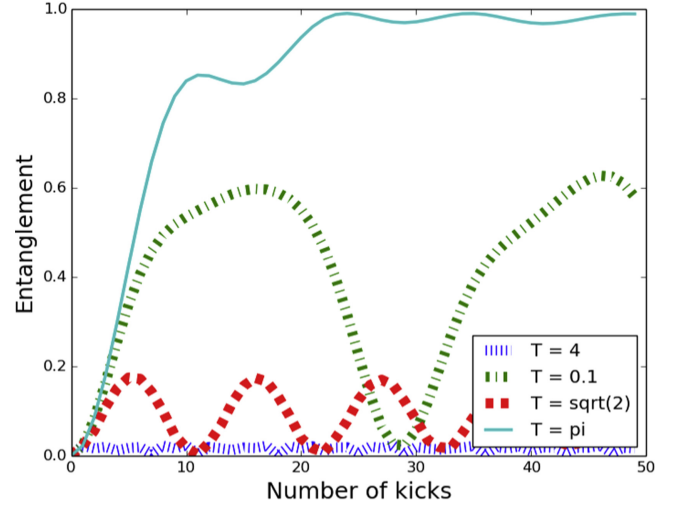


**Figure 3.** Entanglement versus number of kicks for  $V_0 = 0.25$ ,  $\eta = 1/\sqrt{2}$ ,  $T = \pi$  (cyan),  $T = \sqrt{2}$  (red),  $T = 0.1$  (green), and  $T = 4$  (blue). The initial state was taken as a product of the ancilla and Fock state with  $n = 10$ .

Particularly, in the trapped ion context, as  $\hbar_{\text{eff}}$  scales as  $\eta^2$ , i.e.,  $\hbar_{\text{eff}} = \frac{k^2 \hbar}{m\omega}$ , it is easy to vary  $\hbar_{\text{eff}}$  by simply varying the projection of the laser wave vectors on the trap axis [10]. Since entanglement is a genuinely quantum phenomenon, without any classical analog, one could expect that the entanglement degree would diminish as  $\hbar_{\text{eff}}$  becomes negligible. Remarkably, in our numerical simulations we have found just the opposite: entanglement increases faster as  $\hbar_{\text{eff}}$  decreases. This is a surprising result. To observe this counterintuitive behavior we have fixed the other two relevant parameters,  $T$  and  $V_0$ , while varying  $\hbar_{\text{eff}}$ . This result is shown in figure 6 for three values of  $\hbar_{\text{eff}}$  and supported by other numerical simulations (not shown) with different values of  $\hbar_{\text{eff}}$ .

Our numerical results can be understood by looking at the Floquet operator rewritten to include  $\hbar_{\text{eff}}$ : expanding the cosine term one can see that the conditional Floquet operator becomes

$$\mathcal{F} = \exp\left[-iT\left(a^\dagger a + \frac{1}{2}\right)\right] \times \exp\left\{-i\left[\frac{V_0}{\hbar_{\text{eff}}} - \frac{V_0}{2!}(a + a^\dagger)^2 + \frac{V_0}{4!}\hbar_{\text{eff}}^3(a + a^\dagger)^4 - \dots\right] |0\rangle_B \langle 0|\right\}. \quad (14)$$

This result shows that entanglement must saturate for fixed  $V_0$  and sufficiently small  $\hbar_{\text{eff}}$ , since  $\mathcal{F} \rightarrow \exp\left[-iT\left(a^\dagger a + \frac{1}{2}\right)\right] \exp\left\{-i\left[\frac{V_0}{\hbar_{\text{eff}}} - \frac{V_0}{2!}(a + a^\dagger)^2\right] |0\rangle_B \langle 0|\right\}$ , and the conditional operation responsible for entanglement is  $\exp\left\{-i\left[\frac{V_0}{\hbar_{\text{eff}}} - \frac{V_0}{2!}(a + a^\dagger)^2\right] |0\rangle_B \langle 0|\right\} = \exp\left\{-i\left[\frac{V_0}{\hbar_{\text{eff}}} |0\rangle_B \langle 0|\right]\right\} \exp\left\{-\frac{V_0}{2!}(a + a^\dagger)^2 |0\rangle_B \langle 0|\right\}$ . Note that



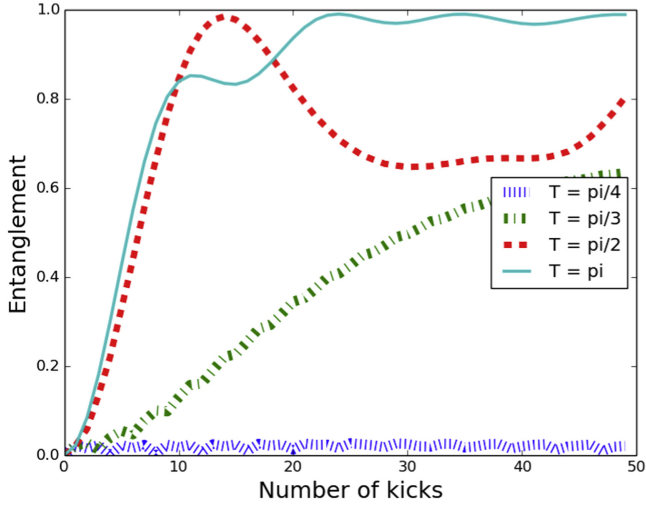


**Figure 4.** Entanglement versus number of kicks for  $V_0 = 0.25$ ,  $\eta = 1/\sqrt{2}$ ,  $n = m = 10$ , and  $T = \pi$  (cyan)  $T = \pi/2$  (red),  $T = \pi/3$  (green),  $T = \pi/4$  (blue). The initial state was taken as a product of the ancilla and Fock state with  $n = 10$ .

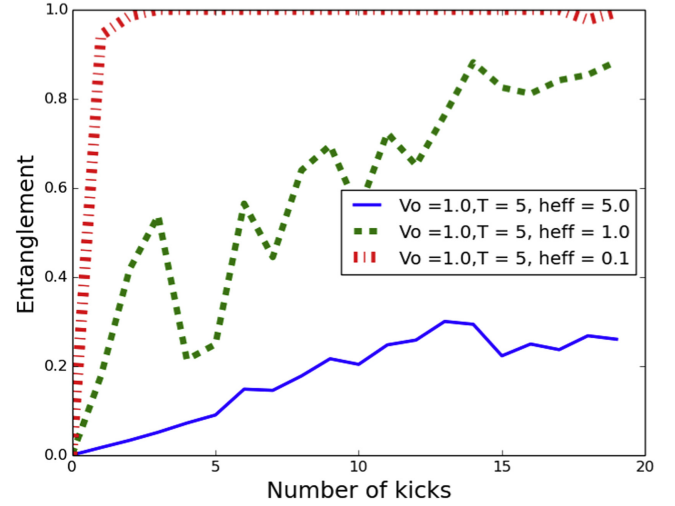


**Figure 6.** Entanglement versus number of kicks for  $T = 5$ ,  $V_0 = 1.0$  and  $\hbar_{\text{eff}} = 0.1$  (red),  $\hbar_{\text{eff}} = 1.0$  (green),  $\hbar_{\text{eff}} = 5.0$  (blue). The initial state was taken as a product of the ancilla and coherent state has  $\alpha = 5$ .

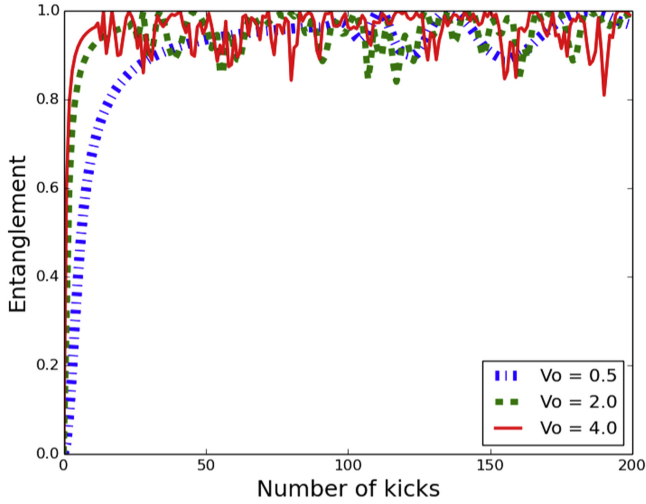


**Figure 5.** Entanglement versus number of kicks for fixed  $\eta = 1/\sqrt{2}$  and  $T = \pi$ ,  $V_0 = 0.5$  (blue),  $V_0 = 2.0$  (green),  $V_0 = 4.0$  (red). The initial state was taken as a product of the ancilla coherent state with  $\alpha = 2$ .

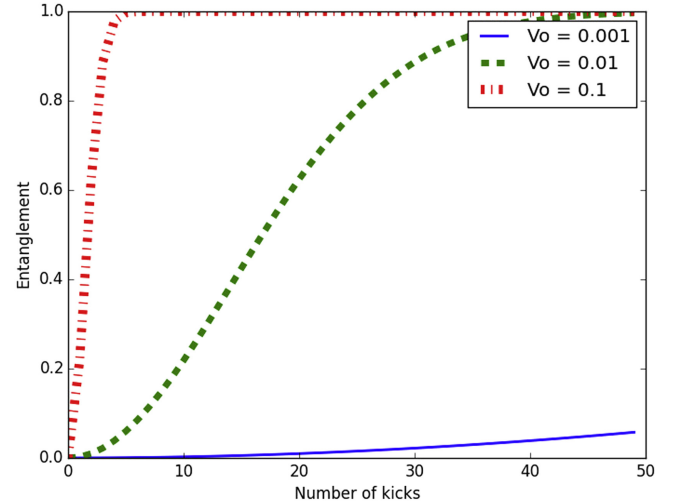


**Figure 7.** Entanglement versus number of kicks for  $\hbar = 0.001$ ,  $T = \pi$ , and  $V_0 = 0.001$  (blue),  $V_0 = 0.01$  (green), and  $V_0 = 0.1$  (red). The initial state was taken as a product of the ancilla and coherent state with  $\alpha = 5$ . The same qualitatively behavior is found for initially Fock states (not shown).

the term  $\exp\left[-i\frac{V_0}{\hbar_{\text{eff}}} |0\rangle_B \langle 0|\right]$  does not produce entanglement, and, as sequentially applied, will just modify the ancilla's relative phase. Therefore, ignoring the conditional phase  $\exp\left[-i\frac{V_0}{\hbar_{\text{eff}}} |0\rangle_B \langle 0|\right]$ , the entanglement is only affected by the term  $\exp\left\{i\left[\frac{V_0}{2!}(a + a^\dagger)^2\right] |0\rangle_B \langle 0|\right\}$ , which is the same irrespective of  $\hbar_{\text{eff}}$ . In other words, when  $\hbar_{\text{eff}} \rightarrow 0$ , entanglement will depend exclusively on the strength of  $V_0$ . Figure 7 shows this behavior for entanglement versus number of kicks using  $T = \pi$ , and three small values of  $V_0$ : 0.001 (solid-blue line), 0.01 (dot-green line), 0.1 (dot-dash- red line), when the quantum KHO is initially in a coherent state with  $\alpha = 5$ . Entanglement production saturates for  $\hbar_{\text{eff}} < 0.001$ , meaning that all the curves coincide, provided that we keep all the

other parameters fixed. We note that our simulations show that increasing  $V_0$  does increase the entanglement faster, achieving its maximum for few kicks (not shown), for initially disentangled ancilla and coherent states. As for example, when  $V_0 = 10$ , saturation occurs for  $\hbar_{\text{eff}} < 0.1$ .

This overall behavior is observed for other initial states, for example in disentangled number states (not shown).

#### 4. Conclusions

In this paper we have investigated, for some initial quantum states, how entanglement behaves as a function of the number

of kicks when varying the three parameters characterizing the quantum kicked harmonic oscillator (KHO), namely the ratio  $T$  between the natural quantum KHO frequency  $\omega$  and the kicking frequency  $\omega_k$ , the coupling strength  $V_0$ , and the effective Planck constant  $\hbar_{\text{eff}}$ . We have found different behaviors to the entanglement depending on the ratio  $T$  being integer or rational, and that the entanglement production is optimized even for few kicks if this ratio is in the crystal condition  $T \in \left\{\frac{\pi}{3}, \frac{\pi}{2}, p\pi\right\}$ ,  $p$  integer. Also, we have found that entanglement increases faster when increasing the strength parameter  $V_0$ . Finally, contrary to what could be expected, we have found that entanglement, a quantum property with no classical analog, increases as  $\hbar_{\text{eff}}$  diminishes, and in the limit  $\hbar_{\text{eff}} \rightarrow 0$  the entanglement production rate saturates, meaning that keeping the other two parameters  $V_0$  and  $T$  fixed, the entanglement dynamics has the same curve, no matter how small we let  $\hbar_{\text{eff}}$  be.

## Acknowledgments

The authors acknowledge financial support from the Brazilian agencies CNPq and FAPPEG. This work was performed as part of the Brazilian National Institute of Science and Technology (INCT) for Quantum Information.

## References

- [1] Zaslavsky G M 1998 *Physics of Chaos in Hamiltonian Systems* (London: Imperial College Press)
- [2] Haake F 2001 *Quantum Signatures of Chaos* 2nd edn (Berlin: Springer)
- [3] Smith A, Anderson B E, Ghose S and Jessen P S 2009 *Nature* **461** 768
- [4] Madhok V, Gupta V, Trottier D-A and Ghose S 2015 *Phys. Rev. E* **91** 032906
- [5] Wimberger S, Mannella R, Morsch O and Arimondo E 2005 *Phys. Rev. Lett.* **94** 130404
- [6] Fromhold T M *et al* 2001 *Phys. Rev. Lett.* **87** 046803
- [7] Gardiner S A, Cirac J I and Zoller P 1997 *Phys. Rev. A* **79** 4790
- [8] Kells G A, Twamley J and Heffernan D M 2004 *Phys. Rev. E* **70** 015203(R)
- [9] Ulf Martin Engel, *On Quantum Chaos, Stochastic Webs and Localization in a Quantum Mechanical Kick System* Nichtlineare und Stochastische, Physik, Bd. 11 ([http://m-engel.de/m\\_engel\\_diss\\_2ol\\_12h/](http://m-engel.de/m_engel_diss_2ol_12h/)) (accessed 11 November 2015)
- [10] Carvalho A R R, de Matos Filho R L and Davidovich L 2004 *Phys. Rev. E* **70** 026211
- [11] Duffy G J, Mellish A S, Challis K J and Wilson A C 2004 *Phys. Rev. A* **70** 041602(R)
- [12] Yeo I *et al* 2014 *Nat. Nanotechnol.* **9** 106–10
- [13] Montinaro M *et al* 2014 *Nano Lett.* **14** 4454–60
- [14] Gloppe A *et al* 2014 *Nat. Nanotechnol.* **9** 920–6
- [15] Jöckel A *et al* 2015 *Nat. Nanotechnol.* **10** 55–9
- [16] Luo S 2003 *Phys. Rev. Lett.* **91** 180403
- [17] Carvalho A R R and Buchleitner A 2004 *Phys. Rev. Lett.* **93** 204101
- [18] Billam T P and Gardiner S A 2009 *Phys. Rev. A* **80** 023414
- [19] Steck D A, Oskay W H and Raizen M G 2001 *Science* **293** 274
- [20] Moore F L *et al* 1995 *Phys. Rev. Lett.* **75** 4598
- [21] Prange R E and Fishman S 1989 *Phys. Rev. Lett.* **63** 704
- [22] Ryu C *et al* 2006 *Phys. Rev. Lett.* **96** 160403
- [23] Schwartz T, Bartal G, Fishman S and Segev M 2007 *Nature* **446** 52
- [24] Lemos Gabriela B, Gomes R M, Walborn S P, Ribeiro P H S and Toscano F 2012 *Nat. Commun.* **3** 1211
- [25] Girolami D, Tufarelli T and Adesso G 2013 *Phys. Rev. Lett.* **110** 240402